This document is the accepted manuscript version of the following article: Quandt, B. M., Braun, F., Ferrario, D., Rossi, R. M., Scheel-Sailer, A., Wolf, M., … Boesel, L. F. (2017). Body-monitoring with photonic textiles: a reflective heartbeat sensor based on polymer optical fibres. Journal of the Royal Society Interface, 14, 20170060 (10 pp.). https://doi.org/10.1098/rsif.2017.0060

Article type: Full Paper

Body-monitoring with photonic textiles: a reflective heartbeat sensor based on polymer optical fibers

*Brit M. Quandt, Fabian Braun, Damien Ferrario, René M. Rossi, Anke Scheel-Sailer, Martin Wolf, Gian-Luca Bona, Rudolf Hufenus, Lukas J. Scherer, Luciano F. Boesel**

Brit M. Quandt, Dr. René M. Rossi, Prof. Dr. Gian-Luca Bona, Dr. Rudolf Hufenus, Dr. Lukas J. Scherer, Dr. Luciano F. Boesel

Empa, Swiss Federal Laboratories for Materials Science and Technology, Lerchenfeldstrasse 5, 9014 St. Gallen, Switzerland

E-mail: Luciano.boesel@empa.ch

Brit M. Quandt, Prof. Dr. Gian-Luca Bona

ETH Zurich, Swiss Federal Institute of Technology, Department of Information Technology and Electrical Engineering, Gloriastrasse 35, 8092 Zurich, Switzerland

Dr. Damien Ferrario, Fabian Braun

CSEM, Swiss Center for Electronics and Microtechnology, Rue Jaquet-Droz 1, 2002 Neuchâtel, Switzerland

Dr. med. Anke Scheel-Sailer

Swiss Paraplegic Center, Guido A. Zäch Strasse 1, 6207 Nottwil, Switzerland

Prof. Dr. Martin Wolf

Biomedical Optics Research Laboratory, Dept. of Neonatology, University Hospital Zurich, Frauenklinikstrasse 10, 8091 Zurich, Switzerland

Keywords: long-term monitoring, polymer optical fibers, photoplethysmography, melt-spinning, biomedical optics

Knowledge of the individual's skin condition is important for pressure ulcer prevention. Detecting early changes in skin through perfusion, oxygen saturation values, and pressure on tissue and subsequent therapeutic intervention could increase the patients' quality of life drastically. However, most existing sensing options create additional risk of ulcer development due to further pressure on and chafing of the skin. Here, as a first component, we present a flexible, photonic textile based-sensor for the continuous monitoring of the heartbeat and blood flow.

Polymer optical fibers (POFs) are melt-spun continuously and characterized optically and mechanically before being embroidered. The resulting sensor shows flexibility when embroidered into a moisture-wicking fabric, and withstands disinfection with hospital-type laundry cycles. Additionally, the new sensor textile shows a lower static coefficient of friction (COF) than conventionally-used bedsheets in both dry and sweaty conditions versus a skin model. Finally, we demonstrate the functionality of our sensor by measuring the heartbeat at the forehead in reflection mode and comparing it with a commercial finger PPG for several subjects. Our results will allow the development of flexible, individualized, and fully textile integrated wearable sensors for sensitive skin conditions and general long-term monitoring of patients with risk for pressure ulcer.

199 words

1. Introduction

Many complex health conditions, e.g. pressure ulcer prevention, require unobtrusive long-term monitoring to register developing wounds early. The changes in skin and underlying tissue vary strongly between individuals and not much data is available so far. People prone to development would benefit from individual feedback and personalized therapeutic intervention. Information on the perfusion of the skin, the oxygen saturation, and pressure levels on the tissue could allow for understanding on tissue changes over time. With long-term data on all three of those parameters, the intervention protocol could then be adjusted to the individual's pressure tolerance curve (depending *e.g.* on the breakdown of microvasculature).(1)

While these diseases need supervision, hospitals often do not have the capacity to monitor these patients at all times.(2) Additionally, the available flexible options (e.g. incorporated printed circuit boards) are often still bulky and cannot be used as they create additional pressure spots and skin chafing.(1, 3, 4) These pressure spots then increase the risk of injury. Additional threats to skin health, including irritation, injury and inflammation have to be avoided. With these prerequisites, the development of textile sensors for long-term measurements becomes essential.

Therefore, we present one component of such a flexible monitoring tool: a photonic textile sensor logging the heartbeat via a PPG (photoplethysmography) signal. This sensor is specifically designed for sensitive skin to prevent (further) injury by only incorporating soft polymer optical fibres (POFs). Recently, development regarding polymer optical fibers for healthcare monitoring has increased greatly.(5) The decreased attenuation adds to the advantage of often higher flexibility compared to glass fibers.(6, 7) As POF can possess yarn-like flexibility, much more flexible and drapeable sensors can be produced and incorporated into textiles.(8, 9) Development of another sensor important to this application – a flexible, pressure-sensitive polymer optical fibre – has recently been published elsewhere.(9)

This textile production requires not only high flexibility of the fibers but also toughness to continue guiding light after production of the textile. Therefore, we present the development and optimization of bi-component polymer optical fibers by continuous melt-spinning, a fast process rendering

continuous fibers. The co-extruded sheath serves here as the optical cladding to a step-index profile POF. Therefore, when discussing the application, the traditional term for POF, cladding, is used.

The heartbeat sensors were produced by embroidery which ensures small bending radii and strong bend light out-coupling from the POFs.(5, 8) The increased light intensity allows for a stronger photoplethysmography (PPG) signal through the tissue. Due to the improved optical properties of these POFs, we were able to verify a the previously used laser light sources were omitted for commercial LEDs, eliminating laser safety restrictions.(8)

Besides light in- and out-coupling, comfort is another important property for textile sensors. Earlier work demonstrated a good correlation between the friction coefficient and the tactile impression.(10, 11) Additionally, it has to be kept in mind that an entirely textile structure will produce a different skin climate than a non-breathable rigid sensor. The wearing comfort, including the transport of sweat away from the skin, can be expected to differ. The removal of fluids from the skin is beneficial for ulcer prevention, especially when having the development of COF from dry to wet state in mind.(12)

Finally, reusability is another important factor in sensor development. The possibility of reusing a sensor makes it economically and ecologically more favourable with decreasing the per-patient cost drastically. Hence, a reusable, washable sensor decreases health cost such targeting a current issue in household spendings.(13) In the medical sector, safe hygienic conditions have to be ensured which then limits development to washable sensors.(14)

The newly-developed fabrics are evaluated in friction and hence dermatologic tolerance. This is performed in comparison to its substrate and other reference textiles against a commercially-available skin model. The sensor is designed to work in reflection mode. This set-up does not require light transmission and can hence be used on any body parts. In the last years we have presented a range of photonic textile sensors for the long-term monitoring of pressure, breathing rate, and heart rate.(8, 15, 16) The latter two have successfully been validated against commercial devices, with a good correlation in acquired data. The heart beat sensor, however, still presents some drawbacks limiting its effective use in clinics: The in-coupling of light into the tissue is done by using a conventional PMMA optical fiber, which is stiff and cumbersome when integrated into the textile.(8) It may therefore lead to low comfort due to high friction and/or skin chafing. Therefore, only the flexible specialty POFs are

used for the new design. The functionality of the sensor is additionally tested after hospital-type washing cycles to guarantee its reusability. For existing wounds, the sensor can be used to determine skin perfusion, which gives information on wound healing.

2. Experimental Section

This paper comprises the development of a textile heartbeat sensor from the production of the sensing component, the POFs, to the subject testing of the sensor. This comprises melt-spinning of a bi-component fibre, evaluation of these in homogeneity, as well as optical and mechanical properties, textile integration, comfort evaluation, and testing. “Comfort” is, in this case, defined by the static coefficient of friction since the targeted patient group typically adheres to strict safety standards to prevent skin chafing.

Melt-spinning of optical fibers

For the production of the bi-component polymer optical fibers, a continuous fiber spinning process was used.(17, 18) The core-cladding-structure was produced by simultaneously spinning two polymers with a melt-spinning plant by Fourné Polymertechnik (Alfter-Impekoven, Germany).(17) Two single screw extruders (18 x 25D for the core and 13 x 25D for the sheath) were used to process and force the two polymers through a bi-component die with inner diameter 1.2 mm, containing a capillary with 0.7 mm outer and 0.4 mm inner diameter. The fiber was cooled in a quenching chamber and three godets were used for drawing. Fiber collection was carried out with a winder as described in a previous publication.(19) The draw ratio, namely the ratio between the winder speed and that of the take-up godet, was varied between 1 and 2.

The core polymer Zeonor 1020R (COP) was acquired from Zeon Chemicals (Louisville, Kentucky, USA), while the sheath polymer THVP-2030G X (THV) is produced by Dyneon GmbH & Co. KG (Burgkirchen, Germany). Their densities are given as 1.01 g/cm^3 and 1.98 g/cm^3 respectively. Before usage, the COP and THV were dried at 100 °C and 90 °C respectively in a vacuum oven for at least 12h. During production, their temperatures at the die were both 250 °C. Further specifications can be taken from **Table 3**.

During the melt-spinning process, light attenuation was monitored for processing changes with a medical laser diode at 652 nm at an intensity of 100 mW (Applied Optronics, South Plainfield, NJ, USA) using the cutback method. The fibers were connected to a mode mixer via F-SMA connectors (Thorlabs, Newton, NJ, USA). The output was logged by using an integrating sphere UM-150 (Gigahertz-Optik GmbH, Türkenfeld, Germany) and a photomultiplier tube (PRC Krochmann, Berlin,

Germany). Optimization of production parameters was performed iteratively to receive low-loss fibers and improve previously produced fibers regarding homogeneity and mechanical performance.(8, 17)

Homogeneity and mechanical characterization of the optical fibers

The fibers were evaluated in homogeneity by scanning electron microscopy (SEM) (Hitachi S-4800, Hitachi, Ltd., Tokyo, Japan) after being embedded in epoxy, polished perpendicularly, and afterwards coated with Gold-Palladium (10 nm) with a Leica EM ACE600 high-vacuum sputter coater (Leica Microsystems, Wetzlar, Germany). The SEM was operated with a voltage of 5 kV and 10 µA beam current. Additionally, cross-sections, prepared without the coating, were evaluated under a Keyence VHX-1000 Multiscan microscope (Osaka, Japan).

The tensile properties of the fibers were evaluated with the Statimat ME+ (textechno Herbert Stein GmbH & Co. KG, Mönchengladbach, Germany) with a 100 N load cell at 600 mm/min drawing speed. The measurements for each fiber type were repeated 20 times. Hence, the standard deviation of the nominal stress was calculated by error propagation taking the standard deviation of both the initial fiber radius and the variation along the fiber axis into account.

Two further experiments were performed in relation to the mechanical performance of the fibres: Knot efficiency as well as bending resiliency. The knot efficiency was used to determine whether these fibres can be used for embroidery. For bending resiliency, however, the recovery was important for determining whether plastic deformation takes place during embroidery. Plastic deformation of the fibre increases light out-coupling at that location. The knot efficiency was also tested on the same machine with 20 repetitions. For knot efficiency, the ratio of the strength at break of a knotted fiber and the virgin fiber are compared. The knots were pre-tensioned by applying a 25 g weight which lies below the tensile modulus of both fibers. It was not necessary to differentiate between Z- and S-knots as the POF shows no yarn twist. To measure resiliency of the fibers under bending, a lever was lowered onto a horizontally placed fiber end. The end is gradually bent down by the lever at a bending radius of 3 mm and finally released. The fiber end then returned from a bent state towards its initial position. This movement was recorded by a high speed camera and resiliency was calculated from

angle differences between initial and current position at different time frames.(20) For these experiments, a Zwick Z100 with a 100 N load cell was used (Zwick Roell Group, Ulm, Germany).

Attenuation spectra of optical fibers

Optical fiber attenuation spectra were measured by cutback method using an Andor Shamrock spectrograph 303i-A (Andor Technology Ltd., Belfast, UK) equipped with a high-speed CCD camera (iDus DV 420A-OE, Andor). With a 20 µm slit setting and 750 nm centering, the measured range is 465.2 – 1034.1 nm. The lamp SLS201/M (Thorlabs Inc., Newton, NJ, United States) provides 300 – 2600 nm wavelengths with a stabilized tungsten-halogen light source. Additionally, an optical density filter of 2.0 and a 550 nm long-pass filter (ND20B and FGL550, both Thorlabs) were added at the source. The spectra were hence taken from 600 – 1000 nm, 600 nm showing full transmittance through the long-pass filter.(21) Connection to the device under test (DUT) was ensured by two commercial optical fibers (type M14L02 (50 µm diameter) and type M25L02 (200 µm diameter), both Thorlabs). Both fibers were unjacketed, spliced, and connected to the DUT with a droplet of index-matching liquid. The light intensity was maximized by aligning both xyz-stages in regard to the tested fiber. The schematic can be seen in **Figure S 1** (left). The determination of fiber axis for optimized fiber coupling takes the difference of fiber diameters into account (LabVIEW program (National Instruments Switzerland GmbH, Ennetbaden, Switzerland) written by Eugen Zgraggen).(22) A schematic of coupled power at different scanning positions can be seen in **Figure S 1** (right).

Spectrometer data was then recorded at the highest possible integration time without saturation (≤ 60000 counts) for optimum signal-to-noise ratio.

Sensor embroidery

Embroidery was performed on a low-friction bedsheet (Schoeller Textil AG, Sevelen, Switzerland) as a substrate. This textile was designed for decubitus ulcer prevention and hence deemed a suitable substrate for this study.(23) A Saurer Era (SAURER Inc., Arbon, Switzerland), provided by Forster Rohner AG, textile innovations (St. Gallen, Switzerland), was used. The textile was tensioned to a size of 108.1 % and 105.3 % in x- and y-direction respectively with appropriate scaling to the correct

pattern size after release. Additionally, yarn tension of both bobbin yarn (Pes 80/2 textured) and POF (monofilament ID-1144) was monitored.

Friction analysis of the sensor

The skin-fabric interface is simulated by the developed fabric with a mechanical skin model.(24) For the model, Lorica soft® (Lorica Sud, Milan, Italy) was applied as it corresponds well to the roughness and surface topography of human skin.(25) For each measurement, a new skin model was used. The samples were tested for 1000 cycles at a load of 8.5 N (= 13.3 kPa) which lies within the range of typical interface pressures at the ischial tuberosities.(1) The mean static coefficient of friction was calculated by averaging 50 cycles and four repetitions per condition. The stroke length was 20 mm with an oscillation frequency of 1.25 Hz.

For the friction measurements, three different designs were used. The embroidered structures covered 64.4 %, 80.2 %, and 100 % (6.4 cm^2) of the measurement patch. The additional measurements in wet conditions were performed by applying 64 µL of deionized water on the skin model to simulate extreme moisture (e.g. heavy sweating).(26) All tests were performed in standard climate conditions (20±1 °C, 65±2 %RH).

Washing tests of the sensor

Evaluation of the sensor was done both through side light out-coupling intensity as well as monitoring the cross-sections of the fibers, the latter also being evaluated statistically in **Table 1**.

Laundry tests were performed on a Roaches Washtec-P TPC 3002 (Birstall, England) according to the protocol given by EN ISO 105-C06:1997 A1M at 40 °C for 45 min, the effective temperature of the detergent. A hospital grade industrial powder detergent was used containing oxygen bleach.(27) The sample was washed with 4 g detergent per litre deionized water within a plastic bottle. The sample holder was attached to a rotating shaft that immersed the sample into the heated water tank. After washing, the sample was removed from the solution, rinsed with deionized water and dried at air.

The normalized light out-coupling intensity from a red LED (λ_{peak} = 660 nm, E97, Industrial Fiber Optics, Tempe, Arizona, USA) was evaluated along the embroidered lines with an optometer (P9710,

Gigahertz-Optik GmbH, Türkenfeld, Germany) as seen in **Figure 3 (a)**. The measurements were repeated 5 times to take connector variability into account. Propagation of error was considered for the standard deviations in determining the light emission over the entire textile. The used detector covers from 400-1000 nm (RW-3705-2, SN21103).

Heartbeat sensor testing

The produced sensor (**Figure 5**) was tested with dedicated electronics based on the PPG acquisition chain. Photoplethysmography detects blood volume changes by utilizing the absorption of light by hemoglobin. At larger blood volumes (e.g. with each heart beat), a signal reaching the detector is decreased. The waveform shows the pulsatile component of the heart beat while being superimposed on a baseline. The former is caused by the changes with each heart beat while the latter is caused by lower-frequency components.(28, 29) The connection between the electronic and the optical fiber was obtained using a commercial infrared LED (λ=870) and a phototransistor (gain of 100 A/W) from Industrial Fiber Optics (Tempe, Arizona, USA), part IF-E91D and IF-D92 respectively. The heartbeat was recorded from the forehead in reflection mode. The sensor was fixed to the head with a headband. The measurement protocol for comparison of the sensors included recording of a baseline (1 minute), two isometric handgrip exercises at approximately 40 % maximum voluntary contraction over 1 and 1.5 minutes as well as 1.5 minutes of deep breathing, both leading to modulation of heart rate. The subject was sitting on a chair and reference heart beat was synchronously measured with a fingertip PPG sensor connected to the BIOPAC MP150 (Biopac Systems Inc., USA). The verification was repeated for 5 subjects.

Statistical data analysis

Statistical data analysis was performed on acquired data with the “R" program and the “R-commander" package.(30, 31) Shapiro-Wilk tests were used to test for the normality of the samples; afterwards differences in the central values of two samples were tested by using the Student *t* test (for samples following the normal distribution) or the Mann-Whitney *U* test (otherwise). One-way analysis of variance (ANOVA) was used to test for differences in means of groups of samples following the

normal distribution, with Tukey Contrasts being subsequently used for the multiple comparisons of means. In case of non-normal samples, we applied the Kruskal-Wallis Rank Sum tests and Pairwise Wilcoxon Rank Sum tests, respectively. The analysis results are noted at the respective images or tables.

3. Results and Discussion

3.1. Homogeneity and mechanical characterization of the optical fibers

We produce two POF fibers, named ID-1143 and ID-1144 via melt-spinning. While the draw ratio of ID-1143 is 1, ID-1144 is drawn to a ratio of 2. Both fibers show good roundness with a flattening of maximum 4.5 % of both core or optical cladding. However, with the flattening of the core significantly lower for fiber ID-1144 ($p < 0.05$), the interface of core and optical cladding is more homogeneous along the fiber axis. Additionally to the roundness, the core is off-centred within the sheath by only 4.2 µm (ID-1143) and 3.7 µm (ID-1144) (**Table 1**). Deviations in the core weight percentage between produced fibers and the extrusion settings occurred due to gear pump throughput. The throughput is dependent among others on the polymer viscosity. Seeing that the fibers were produced at high temperature, densities of polymers can differ greatly from the data sheet value at room temperature.(32, 33) Therefore, the calculated value from the extruder control deviates from the obtained fibers.

Fiber ID-1144 shows slightly lower standard deviations in both core and optical cladding possibly due to the hot drawing, evening the fiber. The influence of drawing a fiber also carries into the tensile properties. While the drawn fiber shows a much larger tensile modulus, the average elongation at break lies below one third of the undrawn fiber (**Figure 1 (a)**). Both fibers show small error within their tensile properties, underlining their good homogeneity. Fiber ID-1144 shows even lower standard deviation of the elongation at break, possibly due to less spinning instabilities (**Table 2**). These decrease with higher drawing ratio.

The stress-strain graphs (**Figure 1 (a)**) show the upper yield point as well as plastic deformation and subsequent strain hardening starting at ~90 % for ID-1143. Fiber ID-1144 is drawn during production and hence already plastically deformed.(34) After the upper yield point, minor fluctuations between residual plastic deformation and strain hardening can be seen. Additional tests have been performed as can be seen in **Figure S 2** with pre-drawn fibers. With pre-drawn fibers to 26 % strain, these fluctuations are eliminated. For these experiments, the initial radius was adjusted to an average 71.7 µm (since the fibers were elongated). This value was then used for stress calculations.

In the context of its later application area, the knot efficiency of the fibers has also been evaluated. Seeing that both fibers show high knot efficiency (the strength at break of the knotted fiber) above 96 % of the straight one, they were deemed resistant enough for embroidery (**Table 2**). Fiber ID-1143 shows higher resiliency to bending, reaching 100 % within 12 seconds (**Figure 1 (b)**). From this, we can conclude that fiber ID-1143 is not plastically deformed at a bending radius of 3 mm, comparing to sole COP fibers.(20) Even with an optical cladding, the good resiliency of the COP material is preserved. Fiber ID-1144 returns to its maximum value also within 12 seconds, however, it does not recover fully. This speaks for the onset of plastic deformation and hence some plastic deformation during embroidery. The lower resiliency compared to the undrawn fiber could be explained by its drawn state and hence higher stiffness as well as the lower diameter which influences bending stress.

3.2. Attenuation spectra of optical fibers

In order to verify usage of the flexible optical fibers both in visible and near-infrared wavelengths applications, the attenuation spectra were measured via cutback method. The full spectrum can already give information for further applications using several wavelengths e.g. oxygen saturation measurements. **Figure 2** shows the attenuation loss for both fibers. The drawn fiber (ID-1144) shows overall lower attenuation but similar peak positions. Comparing to glass fibers for communication systems as well as PMMA fibers, the attenuation is higher in most regions, however, in such a short transmission range sensor, the flexibility could outweigh even higher attenuation. Still, for an appropriate signal-to-noise ratio, the attenuation should be minimized. The fibers were designed to be extremely flexible and resilient (as discussed in the previous section, **Figure 1**). To this, cyclo-olefins as well as fluoropolymers add with their low moisture uptake.(35) The newly-produced fibers also compare well to our previous study (measured at 652 nm). (17)

Generally, losses stem from either intrinsic or extrinsic absorption. Extrinsic losses increase due to e.g. bubble generation in the core during production, surface roughness, an inhomogeneous interface between core and optical cladding or impurities. Intrinsic absorption in the infrared regions is mainly caused by the characteristic vibration frequencies of atomic bonds. C-C stretching vibrations can be expected from 1000 nm, as can be noted at the upper end of the spectrum.(36) C-H stretching vibrations occur around 550, 630, 740 and 900 nm and can be expected to make an impact on the

attenuation loss.(36, 37) The differing behaviour of the two fibers around 600 nm could arise from C-F vibrations and hence an influence of the optical cladding on the absorption spectrum.(36) With the more pronounced peaks in those regions for ID-1144, we hypothesize that the optical cladding influences this fiber's attenuation more strongly. This could then also be an indicator for a stronger interface of core and optical cladding of ID-1144.

Presence of overtones of UV-range bands, are excluded due to the usage of the 550 nm long-pass filter. Ultimately, regarding the overall polymer optical fibers' attenuation level, scattering usually dominates.(36)

3.3. Laundry of the sensor

The objective of evaluating washing the sensor is to verify that the entire sensor can be reused with the embroidered polymer optical fibers embedded. This quality results in a longer life cycle and discourages continuing the currently often-followed throwaway society. It is hence very important to show that washing of the sensor is possible.

The cross-sections after washing distinctly show the continued existence core and optical cladding structure of the optical fibers (**Figure 3 (c) and (d)**). The statistically significant difference in diameter can be explained by the speed control of the winder, differing slightly for a full (measurement of the initial fiber characteristics) and empty (sensor production) spool. The light out-coupling intensity from the textile increases after the first washing cycle (**Figure 3 (e)**). We explain this by the removal of dust which may have accumulated on the fiber during embroidery and absorbed light. Also, fluid preventing electrostatic charging at the high production speeds is washed off. The removal of droplets is also observed in microscopic images. Additionally, we observed an average of 1 % shrinkage of the textile, decreasing the bending radius slightly.

The decrease for 10 washing cycles is due to the strong entangling and the subsequent disentangling of the optical fiber bundles during washing that connect to the light source and detector (Figure 4 (left)). However, the light intensity after 10 washing cycles still exceeds the virgin fiber set-up and shows the reusability of the system.

The low coefficient of friction, which lies below that of commercial, typically-used textiles in hospital applications, assures the comfort of the sensor for applications in contact with the skin. The reusability

of the sensor by washing renders it a promising candidate for commercialization making the life cycle of the sensor longer.

The use of conventional textile techniques for the production of the sensor also assures its washability. As shown in **Figure 3 (f)**, the POFs are incorporated as a part of the textile patch itself. This fact is responsible for the excellent performance of the sensor even after 10 washing cycles (**Figure 3 (e)**). In comparison, other systems make use of single fibers that are prone to damage during washing cycles.(5, 38)

3.4. Friction analysis of the sensor

First, samples were prepared with varying covering area of POFs. Such, we verified that the introduced fibers ID-1144 act according to Amonton's 2nd law of friction (**Figure 4 (c)**). This law states that irrespective of the embroidered area, the coefficient of friction stays constant.(39) This does not hold true when strong wear plays a role in the contact situation. Hence, we can conclude that the textile sensor is not subjected to strong wear changing the real contact area from cycle to cycle. It is thus only dependent on applied load for both wet and dry conditions. Additionally, 1000 cycles allow for a judgement on the embroidering stability. A strong increase in COF would have spoken for a disassembly of the fibers from the substrate.

In comparison to different textiles conventionally used as bedsheets (cotton and cotton/polyester (50:50)), the POF textiles outperform both. The newly-developed POF textiles can hence be used for risk patients as we can assume lower skin chafing probability. Especially in wet conditions, the water removal capability of the decubitus bedsheet in combination with fluorinated fibers shows a clear advantage.(40) Not only does the bedsheet allow for wicking, but the POFs can even enhance this effect due to their hydrophobicity.(24, 36, 41) When taking the increase of static COF for the bedsheet into account, the POF textile only increases by 0.023 ± 0.007 for fiber ID-1144. In comparison, the decubitus bedsheet increases on average by 0.048 ± 0.004 for the static COF. Such, the substrate contributes most to the difference in COF between wet and dry conditions. For cotton, a pilling effect can be observed, increasing the COF (**Figure 4 (d)**).

3.5. Heartbeat sensor testing

The optical fiber is bent tightly by being wound around the sewing yarn (**Figure 3 (f)**). Hence, the incorporation of the optical fibers within the textile substrate automatically ensures strong light out-coupling. The out-coupled light then passed through the tissue (schematic in **Figure 5 (a)**) and experiences scattering events and absorption by tissue and blood. When detected by the second set of optical fibers, the signal varies with each heartbeat due to the absorption of light by haemoglobin, which is stronger in larger blood volumes. This signal allows the estimation of physiological parameters such as heart rate and heart rate variabilities. **Figure 5 (b)** shows an example of a raw PPG signal measured at the forehead with the optical fibers (reflection mode) and compared to reference measurements from fingertip PPG (transmission mode) and a raw signal plot of ECG electrodes, both measured using BIOPAC. The heart rate was calculated from the timing of the falling slopes of the PPG signals. Prior to comparison, the heart rate was further interpolated to 1 Hz and averaged over 4 second windows. **Figure 5 (c)** shows the comparison of average heart rate when measured with the new textile-integrated optical fiber sensor and the BIOPAC PPG over the entire measurement protocol of one particular subject. The new sensor and the commercial solution were used at the same time and linked to time stamps. The highest deviations stem from motion artefacts at the end of the handgrip exercise. At these, the exhaustion of the subject is more easily transmitted to the head than the other hand (by trembling) since the second hand was placed on a table. When evaluated over the 5 subjects measured, the final performance shows a mean absolute error of 0.38 bpm; hence the small motion artifacts do not impede sensor performance critically. The Bland-Altman analysis shown in **Figure 5 (d)** reveals a good agreement of the fiber-based heart rate estimate when compared to the reference at the fingertip. The confidence interval suggests that the difference between the sensors is not clinically important and the sensors can hence be used interchangeably.

There have been some examples of the measurement of heartbeat by using POFs in recent years.(5, 8, 38) In our previous work, we successfully measured both the heartbeat as well as the oxygen saturation in the blood in reflection mode using embroidered POFs.(8) However, the system still utilised a stiff, commercial PMMA fiber for transporting light to the skin, with negative effects on the comfort of the sensor and limitations due to the inadequate mechanical properties of such fibers. Suaste-Gómez and Hernández-Rivera have also proposed a POF-based heartbeat sensor.(38) In that

case, however, the sensor is used in transmission mode comparable to conventional pulse oximeters. A clip must be placed around the finger which limits the applicability of the sensor in terms of long-term monitoring. Other systems include e.g. embedded prisms for light-guiding or supplying light by silica fibers.(42, 43)

Our proposed system presents therefore several advantages when placed at a well-perfused area compared to the previous ones. The embroidery of soft, flexible POF on a low-friction textile guarantees comfort to the user even after long periods of use or after several friction cycles. Such a characteristic is of paramount importance to e.g. paraplegic patients, to decrease the risk of developing pressure ulcers. The setup is also modular and allows the integration of other POF-based sensors, e. g., pressure sensors in a single textile patch, increasing the usefulness and decreasing the complexity of the system simultaneously.(15)

4. Conclusion

In this paper, we demonstrated the embroidery of melt-spun polymer optical fibers into textile substrates. The bi-component, continuous melt-spinning approach for optical fibers allowed producing homogeneous fibers with the most recent optimization of production parameters. A reliable core-cladding structure essential for optical fiber light transmission was achieved. We were able to also optimize the mechanical properties of our POFs: This ensured fast and reliable embroidery, decreasing the number of fiber breaks. Simultaneous embroidery of several sensors was therefore possible.

Last, we could, for the first time, present low-friction, flexible, embroidered sensors. The sensors were able to measure the heartbeat (and heart rate) in reflection at the forehead using a LED as the light source. This proof-of-principle hence demonstrates the applicability of the sensor in reflection mode at thicker body parts. In our previous work, the light source was a laser diode which introduces safety concerns when used for clinical trials in skin-contact applications.(8) An LED therefore also offers many advantages in terms of miniaturization and energy consumption, which opens the way towards a successful miniaturization and integration of such sensors into conventional textiles such as clothing or seats. Moreover, contrary to ECG-electrodes, such an optical sensor does not require wetting of the skin to acquire the signal which would otherwise change dermal conditions again.

From here, we will add further wavelengths to the electronics to also record oxygen saturation in the tissue. Moreover, the setup is modular and will also allow the incorporation of other sensing units, *e. g.*, pressure sensors. Such textile sensors will play a fundamental role in the long-term monitoring of patients by offering a comfortable, simple, and reliable way of measuring their vital signs.

Authors' contributions

BMQ carried out the lab work and data analysis, drafted the manuscript and carried out fiber production together with RH; FB and DF worked on the used electronics and data acquisition; AS, GLB, RMR, LJS and MW designed and coordinated the study, LFB carried out the statistical analysis and coordinated the study. All authors participated in the manuscript writing and gave final approval for publication.

Acknowledgements

This project is funded by Nano-Tera.ch (within the ParaTex and the ParaTex-Gateway project) with Swiss Confederation financing. Gratefully acknowledged is the support of Andrés Leal (resiliency testing), Siegfried Derler and Gelu-Mariusz Rotaru (friction), Denise Mitrano (washing), and Eugen Zgraggen and Ivan Shorubalko (optical equipment). Additionally, Benno Wüst shall be thanked for his knowledge in fiber spinning.

1. Mak AFT, Zhang M, Tam EWC. Biomechanics of Pressure Ulcer in Body Tissues Interacting with External Forces during Locomotion. In: Yarmush ML, Duncan JS, Gray ML, editors. Annual Review of Biomedical Engineering, Vol 12. Annual Review of Biomedical Engineering. 12. Palo Alto, CA, USA: Annual Reviews; 2010. p. 29-53.
2. May JH, Bazzoli GJ, Gerland AM. Hospitals' responses to nurse staffing shortages. Health Aff. 2006;25(4):W316-W23.
3. Ramella-Roman JC, Ho T, Le D, Ghassemi P, Nguyen T, Lichy A, et al., editors. Monitoring the impact of pressure on the assessment of skin perfusion and oxygenation using a novel pressure device. Progress in Biomedical Optics and Imaging - Proceedings of SPIE; 2013.
4. Makhsous M, Priebe M, Bankard J, Rowles D, Zeigler M, Chen D, et al. Measuring tissue perfusion during pressure relief maneuvers: Insights into preventing pressure ulcers. Journal of Spinal Cord Medicine. 2007;30(5):497-507.
5. Quandt BM, Scherer LJ, Boesel LF, Wolf M, Bona GL, Rossi RM. Body-Monitoring and Health Supervision by Means of Optical Fiber-Based Sensing Systems in Medical Textiles. Adv Healthc Mater. 2015;4(3):330-55.
6. Ziemann O, Krauser J, Zamzow PE, Daum W. POF-polymer optical fibers for data communication: Springer Science & Business Media; 2013.
7. Tanio N, Koike Y. What Is the Most Transparent Polymer? Polym J. 2000;32(1):43-50.
8. Krehel M, Wolf M, Boesel LF, Rossi RM, Bona G-L, Scherer LJ. Development of a luminous textile for reflective pulse oximetry measurements. Biomedical Optics Express. 2014;5(8):2537-47.

9. Quandt BM, Hufenus R, Weisse B, Braun F, Wolf M, Scheel-Sailer A, et al. Optimization of novel melt-extruded polymer optical fibers designed for pressure sensor applications. Eur Polym J. 2017;88:44-55.
10. Ramalho A, Szekeres P, Fernandes E. Friction and tactile perception of textile fabrics. Tribology International. 2013;63:29-33.
11. Bertaux E, Derler S, Rossi RM, Zeng X, Koehl L, Ventenat V. Textile, physiological, and sensorial parameters in sock comfort. Textile Research Journal. 2010;80(17):1803-10.
12. Powers JG, Higham C, Broussard K, Phillips TJ. Wound healing and treating wounds Chronic wound care and management. J Am Acad Dermatol. 2016;74(4):607-25.
13. Reducing cost and improving the quality of health care. https://www.whitehouse.gov/sites/default/files/docs/erp2013/ERP2013_Chapter_5.pdf: The White House; 2013.
14. Soukup R, Hamacek A, Mracek L, Reboun J, editors. Textile based temperature and humidity sensor elements for healthcare applications. Proceedings of the 2014 37th International Spring Seminar on Electronics Technology, ISSE 2014; 2014.
15. Krehel M, Rossi RM, Bona G-L, Scherer LJ. Characterization of Flexible Copolymer Optical Fibers for Force Sensing Applications. Sensors. 2013;13:11956-68.
16. Krehel M, Schmid M, Rossi R, Boesel L, Bona G-L, Scherer L. An Optical Fibre-Based Sensor for Respiratory Monitoring. Sensors. 2014;14(7):13088-101.
17. Reifler FA, Hufenus R, Krehel M, Zgraggen E, Rossi RM, Scherer LJ. Polymer optical fibers for textile applications - Bicomponent melt spinning from cyclic olefin polymer and structural characteristics revealed by wide angle X-ray diffraction. Polymer (United Kingdom). 2014;55(22):5695-707.
18. White WR, Blyler Jr LL, Ratnagiri R, Park M, editors. Manufacture of perfluorinated plastic optical fibers. Optical Fiber Communication Conference, OFC 2004; 2004; Los Angeles, CA.
19. Hufenus R, Reifler FA, Maniura-Weber K, Spierings A, Zinn M. Biodegradable bicomponent fibers from renewable sources: Melt-spinning of poly(lactic acid) and poly[(3-hydroxybutyrate)-co-(3-hydroxyvalerate)]. Macromol Mater Eng. 2012;297(1):75-84.
20. Leal AA, Mohanty G, Reifler FA, Michler J, Hufenus R. Mechanical response of melt-spun amorphous filaments. Sci Technol Adv Mater. 2014;15(3).
21. Thorlabs. Unmounted Longpass Colored Glass Filters: Thorlabs; 2016 [Available from: http://www.thorlabs.de/newgrouppage9.cfm?objectgroup_id=999&pn=FGL550#3709.
22. Zgraggen E. Fabrication and System Integration of Single-Mode Polymer Optical Waveguides. Zurich, Switzerland: ETH Zurich; 2014.
23. Derler S, Rao A, Ballistreri P, Huber R, Scheel-Sailer A, Rossi RM. Medical textiles with low friction for decubitus prevention. Tribology International. 2012;46:208-14.
24. Derler S, Schrade U, Gerhardt LC. Tribology of human skin and mechanical skin equivalents in contact with textiles. Wear. 2007;263(7-12 SPEC. ISS.):1112-6.
25. Gerhardt LC, Schiller A, Müller B, Spencer ND, Derler S. Fabrication, characterisation and tribological investigation of artificial skin surface lipid films. Tribol Lett. 2009;34(2):81-93.
26. Gerhardt L-C, Strässle V, Lenz A, Spencer ND, Derler S. Influence of epidermal hydration on the friction of human skin against textiles. Journal of The Royal Society Interface. 2008;5(28):1317-28.
27. Mitrano DM, Arroyo Rojas Dasilva Y, Nowack B. Effect of Variations of Washing Solution Chemistry on Nanomaterial Physicochemical Changes in the Laundry Cycle. Environ Sci Technol. 2015;49(16):9665-73.
28. Allen J. Photoplethysmography and its application in clinical physiological measurement. Physiol Meas. 2007;28(3):R1-R39.

29. Meredith DJ, Clifton D, Charlton P, Brooks J, Pugh CW, Tarassenko L. Photoplethysmographic derivation of respiratory rate: a review of relevant physiology. J Med Eng Technol. 2012;36(1/2):1-7.
30. R: A Language and Environment for Statistical Computing, (2012).
31. Fox J. The R Commander: A basic statistics graphical user interface to R. Journal of Statistical Software. 2005;14:1-42.
32. ZeonCorporation. Datasheet Zeonor 1020R. http://www.zeon.co.jp/content/200181692.pdfaccessed March 9th, 2016.
33. DyneonLLC. Datasheet THVP 2030 GX. http://multimedia.3m.com/mws/media/623296O/thvp-2030g-x.pdf; accessed March 9th, 2016.
34. Nadella HP, Spruiell JE, White JL. Drawing and annealing of polypropylene fibers: Structural changes and mechanical properties. J Appl Polym Sci. 1978;22(11):3121-33.
35. Khanarian G, Celanese H. Optical properties of cyclic olefin copolymers. OPTICE. 2001;40(6):1024-9.
36. Groh W. Overtone absorption in macromolecules for polymer optical fibers. Die Makromolekulare Chemie. 1988;189(12):2861-74.
37. Zhou M. Low-loss polymeric materials for passive waveguide components in fiber optical telecommunication. OPTICE. 2002;41(7):1631-43.
38. Suaste-Gómez E, Hernández-Rivera D, Sánchez-Sánchez A, Villarreal-Calva E. Electrically Insulated Sensing of Respiratory Rate and Heartbeat Using Optical Fibers. Sensors. 2014;14(11):21523.
39. Cheong WCD, Yong AM. Probing the Complexities of Friction in Submicron Contacts Between Two Pristine Surfaces. In: Sinha KS, Satyanarayana N, Lim CS, editors. Nano-tribology and Materials in MEMS. Heidelberg, Germany: Springer Heidelberg; 2013. p. 199-213.
40. Derler S, Rotaru GM, Ke W, Issawi-Frischknecht LE, Kellenberger P, Scheel-Sailer A, et al. Microscopic contact area and friction between medical textiles and skin. J Mech Behav Biomed Mater. 2014;38:114-25.
41. Rotaru GM, Pille D, Lehmeier FK, Stämpfli R, Scheel-Sailer A, Rossi RM, et al. Friction between human skin and medical textiles for decubitus prevention. Tribology International. 2013;65:91-6.
42. Witt J, Schukar M, Krebber K, Pažoutová H, Demuth J, Santostefano N, et al., editors. Personal protective equipment with integrated POF sensors2013; Krakow.
43. Rothmaier M, Selm B, Spichtig S, Haensse D, Wolf M. Photonic textiles for pulse oximetry. Opt Express. 2008;16(17):12973-86.

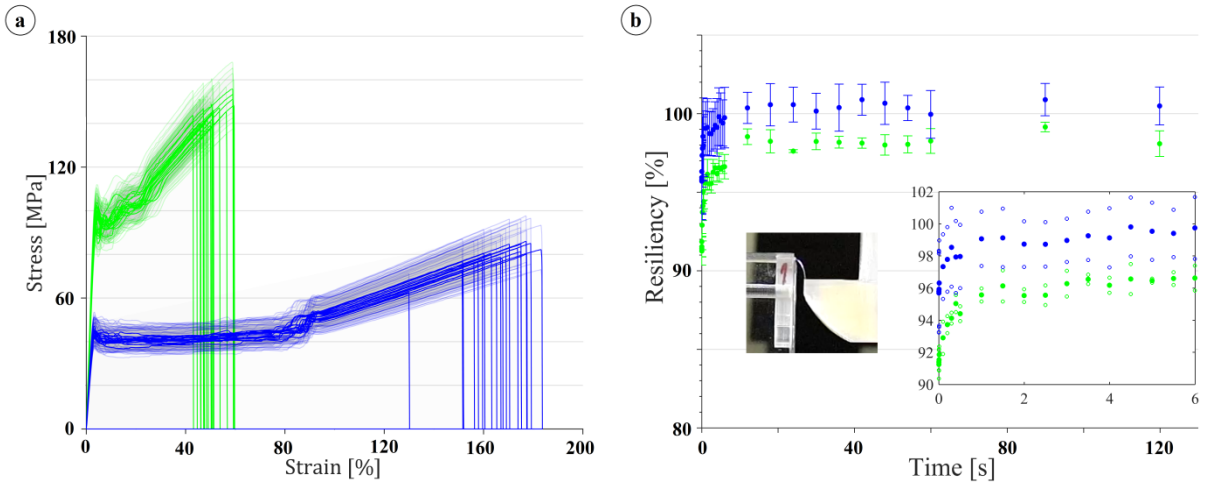

Figure 1: (a) Mechanical testing of the polymer optical fibers ID-1143 (blue) and ID-1144 (green), the plotted standard deviation arises from the error in (initial) radii of the fibers when converting to stress; (b) Resiliency of the optical fibers to bending at a bending radius of 3 mm. Fiber ID-1143 is plotted in blue while fiber ID-1144 is plotted in green. The inset shows the set up at the point just before release of the fiber as well as a plot of the first 6 s of recovery (solid dots), with the lower and upper standard deviation given for each point as well (vacant dots).

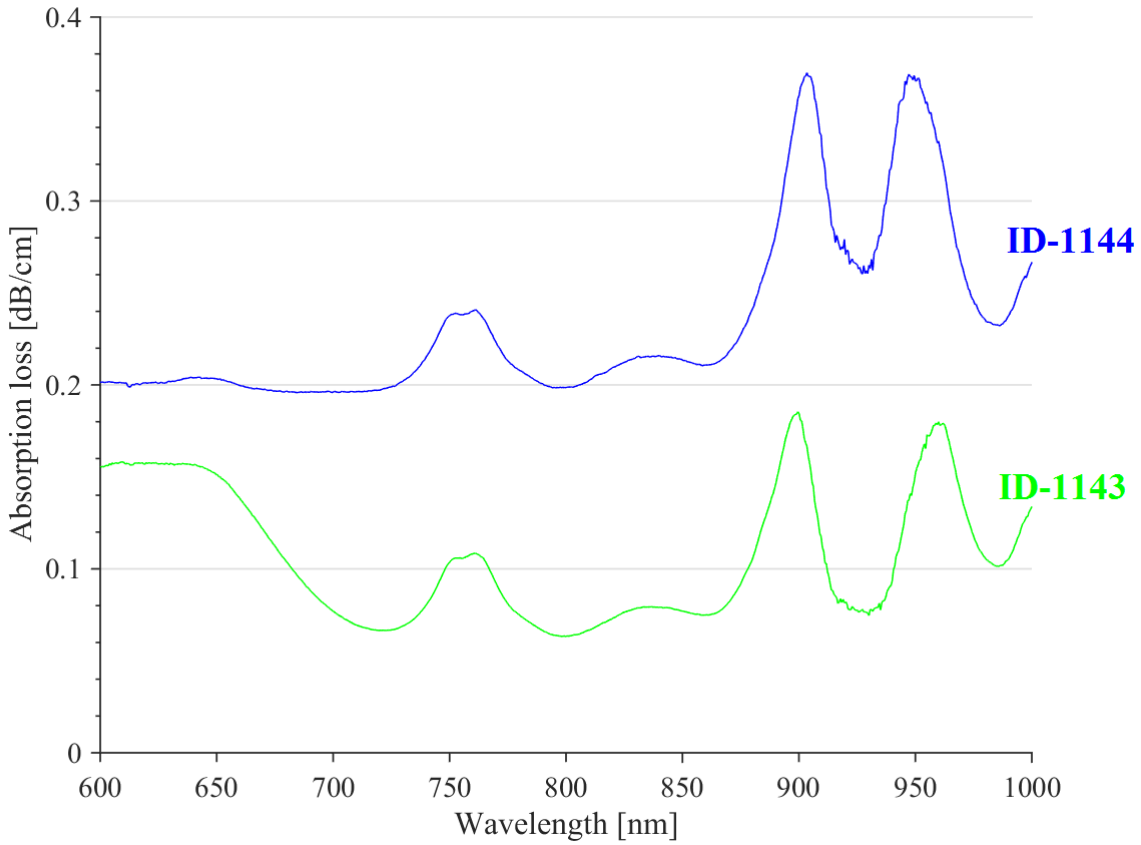

Figure 2: Attenuation spectrum from 600 to 1000 nm for the two polymer optical fibers; ID-1143 is plotted in blue, while ID-1144 is plotted in green.

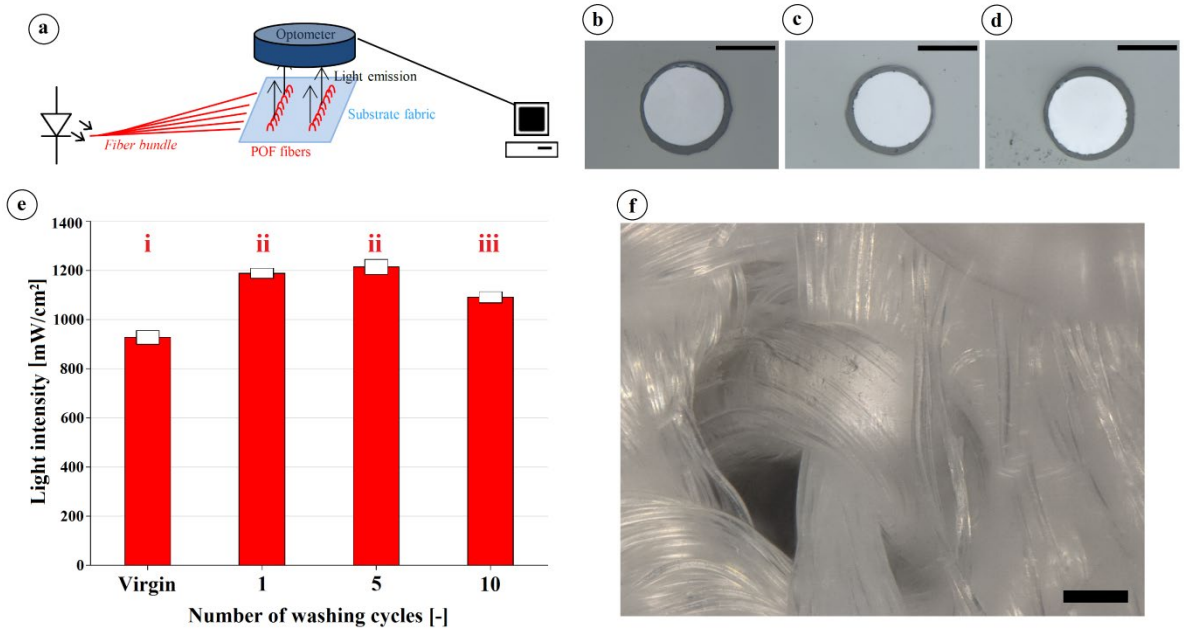

Figure 3: (a) Light out-coupling measurement set-up; Cross-section images of the virgin fiber (b), a fiber washed once without detergent (c), and a fiber washed once with hospital-grade detergent (4g/L) (d); (e) Results for the tested fabric: The intensity is given for the untreated fabric as well as after 1, 5, and 10 washing cycles. The error bars correspond to 5 repeated measurements to correct for connector variation. The superscripts "i, ii, iii" identify samples which do not show significant differences ($p < 0.05$); (f) 3D microscope image of the embroidered polymer optical fiber within the textile. All scale bars indicate 100 µm.

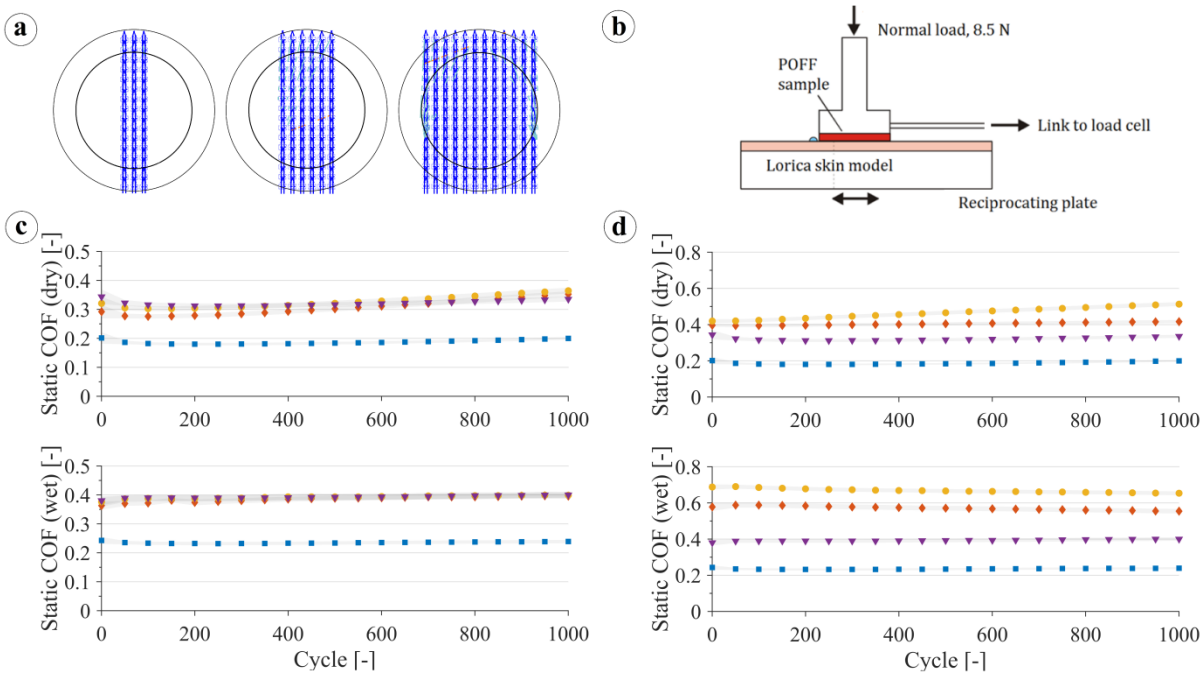

Figure 4: (a) Design for the friction measurements for both optical fibers ID-1144 and ID-1143. The outer circle shows the punched-out area for the friction measurements, the inner circle shows the area in contact with the skin model, (b) Schematic of testing set-up, the POF fabric (POFF) is tested versus a skin model at a normal load of 8.5 N. The coefficient of friction is calculated with the load cell data, adapted from (23) with permission from Elsevier, (c) Static coefficient of friction of fiber ID-1144 in dry (top) and wet (64 µL) (bottom) conditions with varying fiber content on the test patches. Colors/Shapes correspond to the following configurations: three embroidered lines (orange diamonds), six embroidered lines (yellow circles), and twelve embroidered lines (purple triangles) while the substrate (textile without POFs) as a reference is plotted with blue squares; (d) Static coefficient of friction of different textiles in dry (top) and wet (64 µL) (bottom) conditions. The following fabrics are compared: Decubitus bedsheet (Schoeller) (blue squares), cotton/polyester (50:50) (orange diamonds), cotton (100 %) (yellow circles), and the fiber patches with fiber ID-1144 (purple triangles).

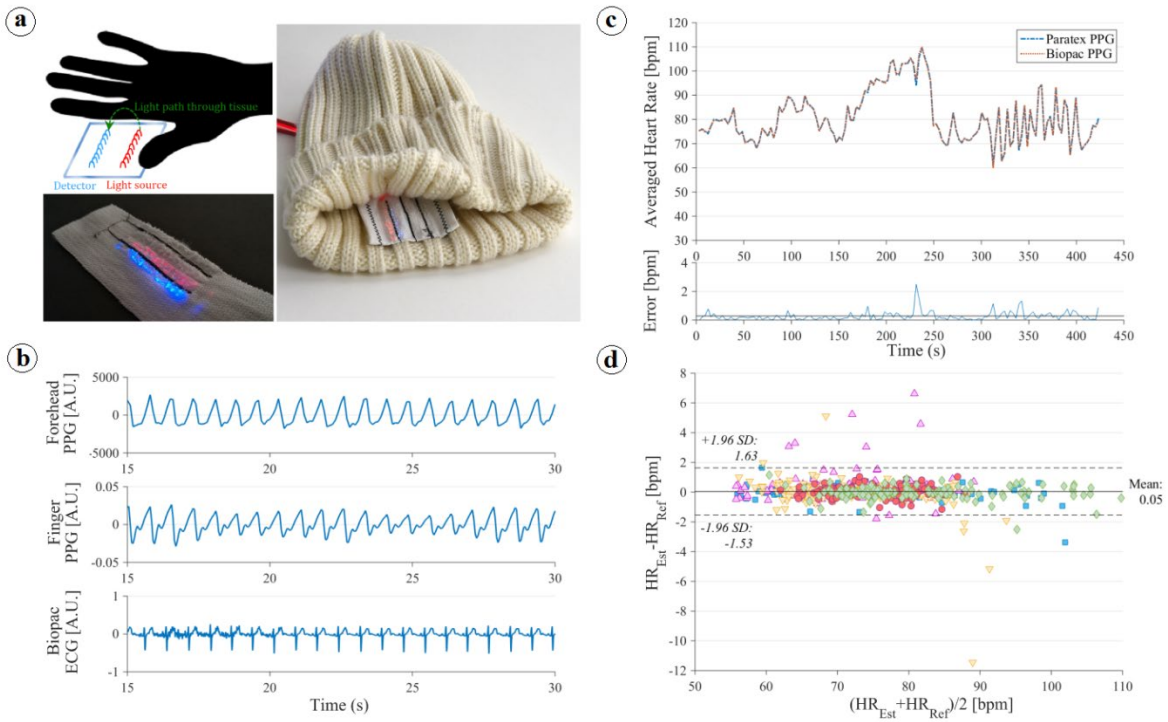

Figure 5: (a) Schematic of the sensing technique of the sensor in reflection mode (upper left), the sensor in close-up while illuminated (emission – red, detection - blue) (lower left), and prototype of the sensing hat (right), (b) raw signals measured with the polymer optical fiber sensor in reflection mode from the forehead, as well as the PPG and ECG signal from the BIOPAC sensors, (c) Calculation of the heartrate averaged over 4 seconds from both, the sensor at the forehead and the BIOPAC finger clip; the average absolute error is given in the lower graph, (d) Bland-Altman plot showing the agreement of the fiber-based sensor (HR_{Est}) and the reference (HR_{Ref}) for 5 subjects (plotted with different colours and symbols).

Table 1: Diameter of core and cladding for virgin and washed optical fibers; for the washed fibers ID-1144, the detergent content varies, either 0 or 4 g/L were used to investigate detergent effect as well. 1) Obtained by SEM images, 2) obtained from optical microscope images. All data regarding fiber ID-1144 was obtained by the same spool of fiber.

	Virgin fiber ID-1143[1]	Virgin fiber ID-1144[1]	ID-1144 – 0g/250mL[2]	ID-1144 – 1g/250mL[2]
Diameter cladding [µm]	179 ± 11 **	161 ± 6 [a]	157 ± 5 [a,b]	156 ± 4 [b]
Diameter core [µm]	156 ± 9 **	141 ± 6 [a]	136 ± 4 [b]	136 ± 3 [b]
Distance centers [µm]	4.2 ± 1.0 *	3.7 ± 1.1 [a]	2.1 ± 0.5 [b]	2.0 ± 0.5 [b]
Flattening cladding [%]	4.0 ± 1.9	4.4 ± 1.9	-	-
Flattening core [%]	4.5 ± 1.7 *	3.7 ± 2.1	-	-
Statistical analysis: i) Fibers ID-1143 x ID-1144: * value significantly different than that for fiber ID-1144 ($p < 0.05$); ** idem ($p < 0.01$). ii) Effect of washing: superscripts "a,b" identify samples (in the same line) which do not show significant differences for the corresponding property ($p < 0.01$).				

Table 2: Tensile properties of both fibers ID-1143 and ID-1144 in their virgin state as well as when knotted with tensioning of 25 g.

	Tensile modulus [MPa]	Ultimate tensile strain [%]	Ultimate tensile stress [MPa]	Knot efficiency [%]
ID-1143	16.9 ± 0.7 [a]	165.6 ± 12.4	79.2 ± 5.3	98.1 ± 0.3
ID-1143 – knotted	12.7 ± 0.8	170.4 ± 14.8	77.7 ± 5.4	
ID-1144	30.1 ± 1.3 [b]	51.1 ± 5.3	144.6 ± 5.0 [b]	95.9 ± 1.4
ID-1144 – knotted	22.7 ± 1.8	49.4 ± 6.9	138.6 ± 6.8	

Table 3: Production parameters of the bi-component polymer optical fibre ID-1143 and ID-1144.

Fiber No.	Polymer		c/s	Core	Godet 1		Godet 2		Godet 3		Winder	Draw ratio
	Core	Sheath	Vol. ratio	wt.-%	Speed [m/min]	Temp. [°C]	Speed [m/min]	Temp. [°C]	Speed [m/min]	Temp. [°C]	Speed [m/min]	
ID-1143	COP	THV	2.0	51	300	40	305	40	310	40	305	1.0
ID-1144	COP	THV	2.0	51	200	40	300	90	400	40	395	2.0

Statistical analysis: The following two-sample comparisons have been performed for the three investigated tensile properties: i) fibers ID-1143 x ID-1144: all properties present significant different values ($p < 0.01$); ii) fibers ID-1143 knotted x ID-1144 knotted: idem; iii) fibers ID-1143 x ID-1143 knotted: properties with significant differences are marked with the superscript "a"; iv) fibers ID-1144 x ID-1144 knotted: idem, superscript "b".

Reporting of an all-textile polymer optical fiber heartbeat sensor concentrating on decubitus research. The optical fibers are characterized optically and mechanically. Dermatologic considerations for risk patients are addressed by friction analyses of the sensor vs. an established skin model. The findings also include economic and ecological examination with washability. The heartbeat is measured in reflection making LED-powered textile photoplethysmography possible.

60/60 words

Keywords: long-term monitoring, polymer optical fibers, skin friction, melt-spinning

Novel textile-integrated optical fiber-based transcutaneous heartbeat sensor for sensitive skin

Brit M. Quandt[1,2], Damien Ferrario[3], René M. Rossi[1], Anke Scheel-Sailer[4], Martin Wolf[5], Gian-Luca Bona[1,2], Rudolf Hufenus[1], Lukas J. Scherer[1], Luciano F. Boesel[1]*

ToC figure – 110 mm broad × 20 mm high

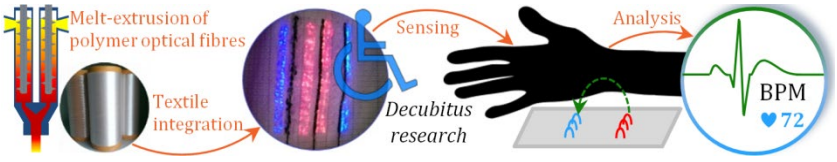

Supporting Information

Novel textile-integrated optical fiber-based transcutaneous heartbeat sensor for sensitive skin

Brit M. Quandt[1,2], Damien Ferrario[3], René M. Rossi[1], Anke Scheel-Sailer[4], Martin Wolf[5], Gian-Luca Bona[1,2], Rudolf Hufenus[1], Lukas J. Scherer[1], Luciano F. Boesel[1]*

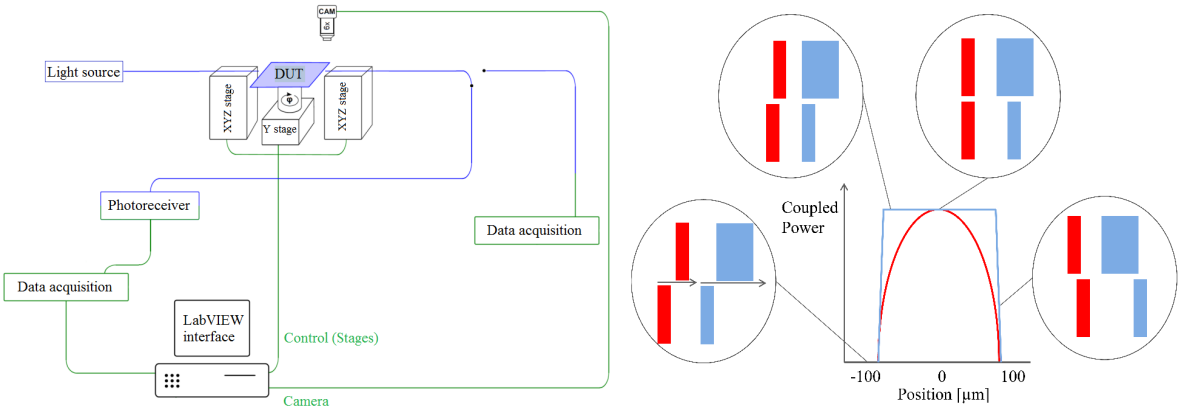

Figure S 1: Schematic of the set-up for measuring light attenuation over a spectrum of 600-1000nm including the aligning mechanism (left). The schematic was adapted from (22), green lines highlight electrical connection whereas blue lines optical ones. The alignment process of the fiber axes is shown for fibers with similar (red) and different (blue) diameters and their respective output at different locations during scanning correlating to the performed fit (right).

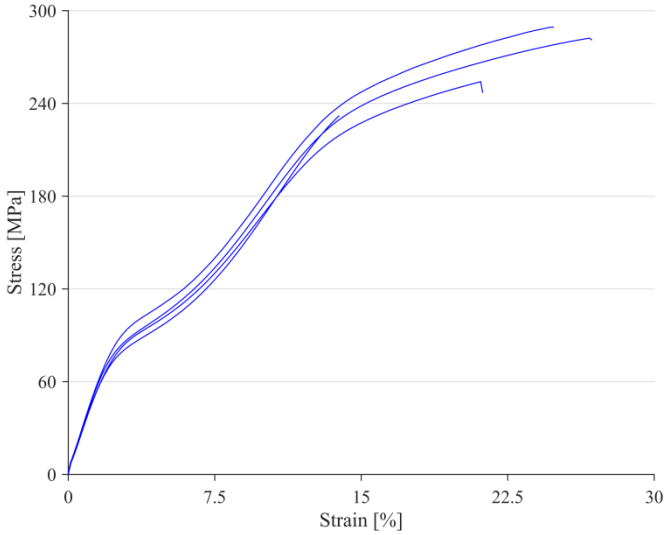

Figure S 2: Mechanical testing of fibre ID-1144 after drawing to 26 % (well within plastic deformation); the initial radius is reduced to 71.7 µm.